Dalton Transactions

ARTICLE

Thorium(IV) Alkyl and Allyl Complexes of a Rigid NON-Donor Pincer Ligand with Flanking 1-Adamantyl Substituents

Nicholas R. Andreychuk,[a] Tara Dickie,[a] David J. H. Emslie,*,[a] Hilary A. Jenkins[a]

Palladium-catalyzed coupling of 1-adamantylamine (2 equiv.) with 4,5-dibromo-2,7-di-*tert*-butyl-9,9-dimethylxanthene afforded the proligand 4,5-bis(1-adamantylamino)-2,7-di-*tert*-butyl-9,9-dimethylxanthene, $H_2[XAd]$ (**1**), which upon deprotonation with excess KH or KCH_2Ph in THF or dme generated $[\{K(THF)_3\}_2(XAd)]$ (**2a**) and $[K_2(XAd)(dme)]$ (**2b**). Subsequent reaction of *in-situ* generated **2a** or **2b** with $[ThCl_4(dme)_2]$ yielded $[(XAd)ThCl_4K_2]\cdot x(dme)$ (**3**; x = 0.5-2), which reacted with 2 equiv. of $LiCH_2SiMe_3$ or $K[allyl^{TMS}]$ to afford the bis(hydrocarbyl) complexes $[(XAd)Th(CH_2SiMe_3)_2(THF)]$ (**4**) and $[(XAd)Th(\eta^3-allyl^{TMS})_2]$ {**5**; $allyl^{TMS}$ = 1-$(SiMe_3)C_3H_4$}. Dialkyl complex **4** was stable at 80 °C for at least 2.5 hours, but decomposed over 4.5 hours at 110 °C. Diallyl complex **5** was stable for hours at 85 °C, and suffered less than 5% decomposition after 10 minutes at 155 °C. At room temperature, averaging of the *syn* and *anti* protons of the allyl CH_2 groups of **5** occurred on the NMR timescale, as a consequence of rapid π-σ-π hapticity changes. Additionally, low temperature ^{1}H and ^{13}C NMR spectroscopy indicates that **5** exists as a rapidly exchanging mixture of two isomers with C_1 and C_2 symmetry. Compounds **2a**, **4** and **5** were crystallographically characterized.

Introduction

Early actinide elements are unique in that they combine lanthanide-like Lewis acidity and large ionic radii with the potential for appreciable covalency (due to greater f-orbital radial extension for actinide vs lanthanide ions), and the accessibility of a broad range of oxidation states (especially for U, Np and Pu).[1,2] These attributes have the potential to endow actinide complexes with unique reactivity profiles, and the relatively low radioactivity and appreciable natural abundance of thorium and uranium make these elements viable for applications in catalysis.[3]

Organometallic complexes play a central role in catalysis, and actinide complexes bearing multiple hydrocarbyl ligands have been shown to exhibit high reactivity, finding application as catalysts for a range of transformations, including alkyne oligomerization, alkene/alkyne hydrosilylation, hydro-amination, hydrothiolation, and hydroalkoxylation, and olefin polymerization (typically upon activation to generate an alkyl cation).[4] Furthermore, extremely challenging catalytic reactions have in some cases been achieved. For example, upon reaction of thermally unstable $[Th(allyl)_4]$ with dehydroxylated alumina, a robust supported catalyst was obtained, capable of both arene hydrogenation and alkane C–H bond activation.[5]

Early examples of robust actinide polyalkyl complexes relied heavily upon carbocyclic supporting ligands, particularly cyclopentadienyl ligands, to impart thermal stability.[2,6] However, multidentate non-carbocyclic supporting ligands can provide steric and electronic profiles that are readily tuned and are complementary to those of carbocyclic ligands. In actinide chemistry, non-carbocyclic ligands have allowed the synthesis of a range of organometallic derivatives, and prominent examples of tridentate ligand-supported polyalkyl or polyallyl complexes are illustrated in Figure 1.[7,8-18,19,20] These ligands range from facially-capping, as in the case of the tris(3,5-dimethylpyrazolyl)-hydroborate monoanion (see a in Figure 1),[7,21] to exclusively meridionally-coordinating, as in the case of our dianionic 4,5-bis(2,6-di-isopropylphenylamido)-2,7-di-*tert*-butyl-9,9-dimethylxanthene ligand (XA_2; see d in Figure 1).[8,10,17]

The XA_2 pincer ligand was designed to provide an uncommonly rigid coordination environment, by virtue of direct attachment of the flanking donor atoms to a tricyclic xanthene backbone. In combination with large f-element ions, this rigid coordination environment enforces tridentate and meridional coordination. Furthermore, ligand rigidity provides the metal with limited opportunities to minimize the effects of steric bulk through changes in the positions of the ligand donor atoms and bulky substituents, relative to the ligand backbone and one another. This ligand platform provided access to a range of organoactinide derivatives, including dialkyl and trialkyl uranium complexes,[16] mixed alkyl/2-pyridyl uranium derivatives,[22] thorium monoalkyl cations,[9,17] and a dication in which thorium is η^6-coordinated to two $PhCH_2B(C_6F_5)_3$ anions.[17] Furthermore, it provided access to organometallic derivatives of high thermal stability. For example, $[(XA_2)Th(CH_2SiMe_3)_2]$ is stable at 70 °C, and decomposed over several hours at 90 °C;[10]

[a.] *Department of Chemistry & Chemical Biology, McMaster University, 1280 Main Street West, Hamilton, Ontario, L8S 4M1, Canada.*

for comparison, $[Th(OC_6H_3{}^tBu_2-2,6)_2(CH_2SiMe_3)_2]$,[23] $[Cp*Th(OC_6H_3{}^tBu_2-2,6)(CH_2SiMe_3)_2]$,[24] and $[\{Me_2Si(C_5Me_4)_2\}Th-(CH_2SiMe_3)_2]$[25] are reported to decompose at 60 °C.
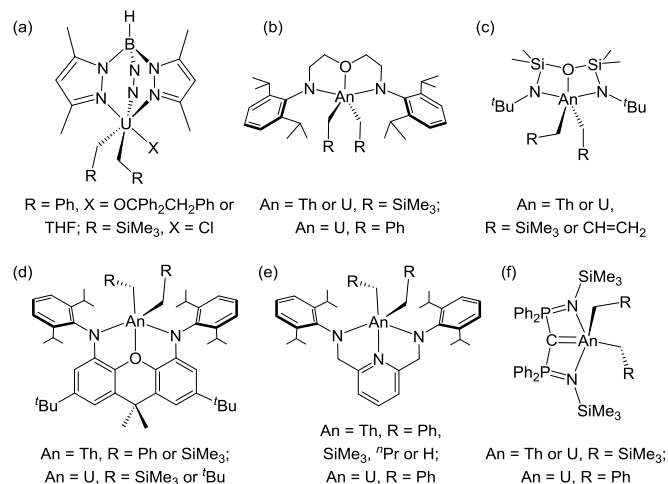
Figure 1. Isolated actinide dialkyl or diallyl complexes supported by a single tridentate ancillary ligand. Examples feature NNN- (a[7] and e[8-11]), NON- (b,[12-14] c (the coordination mode of allyl co-ligands was not conclusively determined),[12,15] and d[10,16,17]) and NCN- (f[18,19]) donor ligands.

A further advantage of ligand rigidity is that modifications to the steric requirements of the ligand should be more predictable, given that substantial alterations in the ligand coordination mode are disfavoured. Herein we explore such a steric modification,[26] via the synthesis of an analogue of the XA_2 ligand in which the flanking 2,6-diisopropylphenyl groups are replaced by 1-adamantyl substituents, and the synthesis of thorium(IV) chloro, alkyl and allyl derivatives of the new ligand. Relative to XA_2, the 4,5-bis(1-adamantylamido)-2,7-di-*tert*-butyl-9,9-dimethylxanthene (XAd) dianion will be a superior donor, with steric bulk positioned in the plane of the xanthene backbone, rather than above and below the plane (Figure 2).
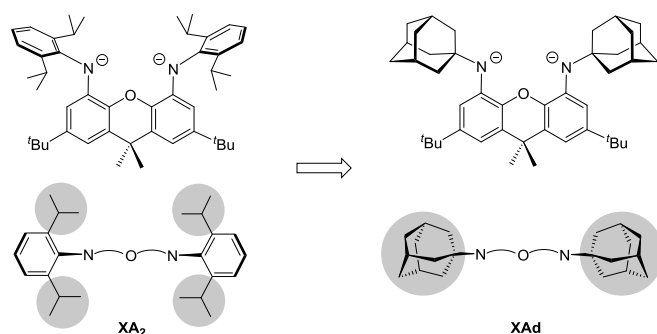

Figure 2. Relationship between the XA_2 and XAd dianions, shown from above (top) and within the plane of (bottom) the xanthene backbone. Shaded areas highlight the positioning of steric bulk relative to the xanthene backbone.

Results and Discussion

The NON-donor proligand, $H_2[XAd]$ (**1**), was synthesized by palladium-catalyzed coupling of 4,5-dibromo-2,7-di-*tert*-butyl-

9,9-dimethylxanthene with 2 equiv of commercially-available 1-adamantylamine (Scheme 1), and was obtained as a white solid in 81% yield upon recrystallization from ethanol/toluene. The $H_2[XAd]$ proligand was then dissolved in toluene and stirred with excess NaH at room temperature, to remove any traces of moisture and ethanol prior to use.
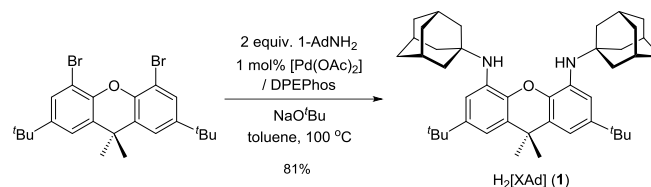
**Scheme 1**. Synthesis of proligand $H_2[XAd]$ (**1**).

In contrast to the reactivity profile of previously reported $H_2[XA_2]$, deprotonation of $H_2[XAd]$ with KH did not proceed rapidly to form an appreciably soluble dipotassium salt in ethereal solvents (e.g. THF or dme). For example, while ether-soluble $[K_2(XA_2)(dme)_2]$ was formed within 5 h via the reaction of $H_2[XA_2]$ with KH in dme at room temperature,[10] deprotonation of $H_2[XAd]$ with excess KH in THF required heating at 65 °C for 72 h, and afforded poorly-soluble $[\{K(THF)_3\}_2(XAd)]$ (**2a**). X-ray quality crystals of compound **2a** were obtained by layering a THF solution of **2a** with hexanes and cooling to −30 °C (Figure 3). In the solid-state, the two potassium atoms of complex **2a** are bound above and below the plane of the XAd ligand backbone, which is significantly planar (the angle between the two xanthene aryl rings is 4.6°). Both potassium atoms are stabilized by a crown of three THF ligands, with the amido and diarylether donors of the XAd dianion in bridging positions between the two potassium cations, forming a distorted square-pyramidal K_2N_2O core with oxygen in the apical site.
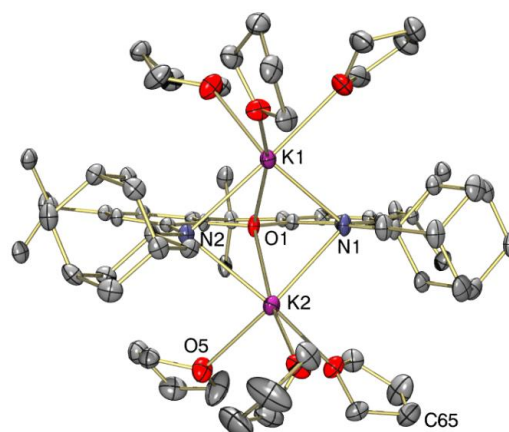
Figure 3. X-ray crystal structure of $[\{K(THF)_3\}_2(XAd)]$ (**2a**), with thermal ellipsoids at 50% probability. Hydrogen atoms are omitted for clarity.

Dipotassium complex **2a** underwent rapid desolvation upon removal of THF solvent *in vacuo*, combined in our hands with unexpected decomposition to yield significant amounts of

H$_2$[XAd] as confirmed by ^{1}H NMR spectroscopy. Alternatively, conducting the reaction of H$_2$[XAd] with KH in dme for 7 days at room temperature yielded highly insoluble [K$_2$(XAd)(dme)] (**2b**; the ^{1}H NMR spectrum of **2b** in THF-d_8 matched that of **2a**, accompanied by 1 equivalent of free dme), but solubility issues precluded isolation of **2b** as an analytically-pure precursor. Compound **2b** can also be prepared more conveniently by stirring H$_2$[XAd] with 2.5 equiv of KCH$_2$Ph for 12 h in dme.
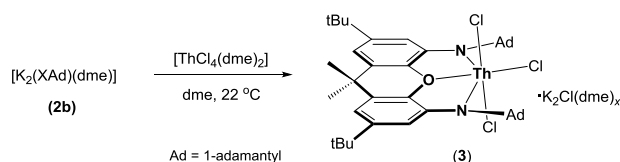
Scheme 2. Synthesis of chloro complex [(XAd)ThCl$_4$K$_2$]·x(dme) (**3**; x = 0.5–2), depicted as a trichloro 'ate' species.

Salt metathesis between *in-situ* generated [K$_2$(XAd)(dme)] (**2b**) and [ThCl$_4$(dme)$_2$] in dme afforded the KCl salt-occluded thorium chloro species [(XAd)ThCl$_4$K$_2$]·x(dme) (**3**), which was isolated as an off-white solid in 64 % yield (for x = 2) after centrifugation, trituration in hexanes, and filtration (Scheme 2). In this complex, dme is not believed to coordinate to thorium, as the amount of dme present varied from batch to batch (x = 0.5-2). Complex **3** was characterized by ^{1}H and ^{13}C{^{1}H} NMR spectroscopy, as well as elemental analysis.

Despite numerous crystallization attempts, only microcrystalline **3** could be obtained. However, the inclusion of two equiv of KCl in **3** was established through multiple elemental analyses, which revealed %CHN values uniformly lower than those expected for salt-free "[(XAd)ThCl$_2$(dme)]". The presence of KCl in complex **3** is additionally suggested by the poor solubility of **3** in aromatic solvents. Leznoff and co-workers observed similar LiCl salt-retention (determined by elemental analysis) in their bis(amido)ether thorium complex [(^{tBu}NON)ThCl$_5$Li$_3$]·dme (^{tBu}NON = {(^{t}BuNSiMe$_2$)$_2$O}$^{2-}$), which was prepared *via* salt metathesis between [Li$_2$(^{tBu}NON)] and [ThCl$_4$(dme)$_2$] in dme.[14]

A thorium dichloride complex, [(XAd)ThCl$_2$]·x(THF)·y(KCl) (**3'**), could also be prepared in THF, and reaction of *in-situ* generated **3'** with 2.1 equiv of LiCH$_2$SiMe$_3$ at 0 °C in THF afforded the neutral, base-stabilized dialkyl complex [(XAd)Th(CH$_2$SiMe$_3$)$_2$(THF)] (**4**; Scheme 3), which was obtained as a white solid in 24% yield after trituration in hexanes and subsequent filtration. Bis(trimethylsilylmethyl) complex **4** is highly soluble in ethereal- and aromatic solvents, and fairly soluble in saturated hydrocarbons.

The room-temperature ^{1}H NMR spectrum of dialkyl complex **4** in C$_6$D$_6$ features twelve resonances between 7.10 and 0.09 ppm, including a single set of sharp ThCH_2 and ThCH$_2$SiMe_3 signals. This is indicative of either: (a) a C_{2v}-symmetric isomer of **4** featuring *trans*-disposed trimethylsilylmethyl groups and a THF ligand coordinated in the plane of the xanthene backbone, or (b) a C_s-symmetric isomer (depicted in Scheme 3) with rapid exchange between axial and in-plane alkyl environments, presumably facilitated by THF dissociation and re-coordination.

The latter explanation was confirmed by observation of a C_s-symmetric structure in the ^{1}H and ^{13}C NMR spectra of **4** at −76 °C.

An X-ray crystal structure of **4** (Figure 4) revealed a six-coordinate XAd-thorium(IV) complex of approximate C_s-symmetry, with one trimethylsilylmethyl group located roughly in the plane of the XAd ligand, one occupying an axial site, and a THF ligand coordinated approximately *trans* to the axial alkyl substituent. The geometry at thorium is best approximated as an edge-capped trigonal bipyramid, with the neutral diaryl ether capping the N(1)⋯N(2) edge of a trigonal bipyramid comprised of the 4 anionic donors {N(1), N(2), C(44), and C(48)} and the oxygen-donor of THF {O(2)}; the N(1)−Th−N(2), N(1)−Th−C(44), N(2)−Th−C(44), and C(48)−Th−O(2) angles are 129.87(7), 112.06(9), 102.68(8), and 172.00(7)°, respectively (τ = 0.70).[27] However, the donor atoms that are bound in the equatorial plane of the distorted trigonal bipyramid {N(1), N(2), and C(44)} are bent toward the axially-bound THF ligand. Consequently, the thorium atom in complex **4** lies 0.54 Å above the N/C(44)/N equatorial plane, and the sum of the N−Th−N and N−Th−C(44) angles is equal to 344.6° (for comparison, the sum of the comparable angles in [(XA$_2$)UMe$_3$]$^-$ is 359.9°).[16]
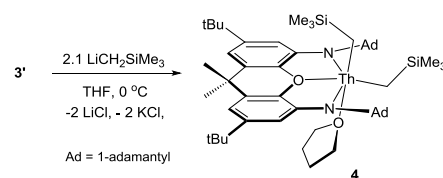
Scheme 3. Synthesis of the dialkyl complex [(XAd)Th(CH$_2$SiMe$_3$)$_2$(THF)] (**4**).
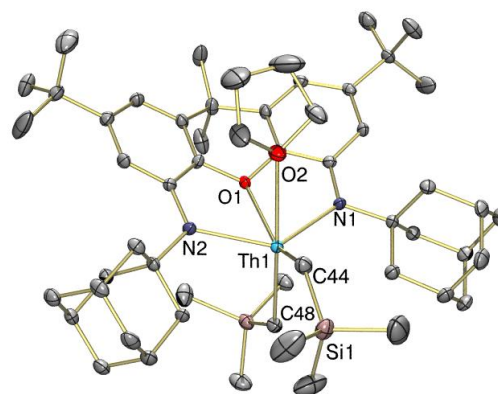
Figure 4. X-ray crystal structure of [(XAd)Th(CH$_2$SiMe$_3$)$_2$(THF)] (**4**), with thermal ellipsoids at 50% probability. Hydrogen atoms are omitted for clarity. The 1-adamantyl methylene carbon atoms closest to thorium are C(25) (of the Ad substituent on N(1)), and C(35) (of the Ad substituent on N(2)).

The xanthene backbone in **4** is also significantly bent away from planarity, with a 32.7° angle between the two aryl rings of the xanthene backbone. This contrasts the situation in six-coordinate actinide complexes of the XA$_2$ ligand (the angle between the aryl rings of the xanthene backbone is 1.2° in [(XA$_2$)UCl$_3${K(dme)$_3$}],[28] 6.5° in [(XA$_2$)UMe$_3$]$^-$, and 4.8 and 7.0° in [(XA$_2$)U(CH$_2$SiMe$_3$)$_3$]$^-$),[16] and likely occurs because xanthene-

bending can be more easily accommodated in the absence of the sterically-restrictive isopropyl groups of the XA$_2$ ligand (located above and below the xanthene backbone; Figure 2).

The Th−N, Th−O$_{xanthene}$, and Th−CH$_2$ distances in complex **4** are expanded by 0.03–0.07 Å relative to those of the corresponding XA$_2$ thorium bis(trimethylsilylmethyl) complex,[10] likely as a consequence of the increased coordination number in **4**, combined with the superior donor ability of the alkylamido donors of XAd. Although structurally-authenticated complexes featuring adamantylamido–thorium linkages have not previously been reported, the Th−N distances in **4** {2.360(2) and 2.368(2) Å} are comparable to those of *tert*-butylamido–thorium species such as [(*^{tBu}*NON)Th(O*^{i}*Pr)$_3$Li(OEt$_2$)] (*^{tBu}*NON = {(*^{t}*BuNSiMe$_2$)$_2$O}$^{2-}$; Th−N = 2.38(1) Å),[29] and [{Me$_2$Si(η^5-C$_5$Me$_4$)(*^{t}*BuN)}Th{N(SiMe$_3$)$_2$}(μ-Cl)]$_2$ (Th−N$_{tBu}$ = 2.335(5) Å).[30] The Th−O$_{THF}$ distance of 2.692(2) Å is relatively long (~ 80% of Th−O$_{THF}$ distances in the Cambridge Structural Database lie within the range of 2.487–2.590 Å),[31] but is comparable to that observed in the six-coordinate triamidoamine thorium complex [(tren^{TBS})ThCl(THF)] (tren^{TBS} = κ^4-{N(CH$_2$CH$_2$NSiMe$_2$*^{t}*Bu)$_3$}$^{3-}$; Th−O = 2.648(9) Å).[32]

The Th−CH$_2$ distances {2.528(3), 2.549(3) Å} in complex **4** are similar to those of the nine additional structurally-characterized examples of neutral thorium trimethylsilylmethyl complexes, namely Marks' metallocene complexes, [Cp*$_2$Th(CH$_2$SiMe$_3$)$_2$] (Th−CH$_2$ = 2.46(1), 2.51(1) Å),[33] and *ansa*-metallocene [{Me$_2$Si(η^5-C$_5$Me$_4$)$_2$}Th(CH$_2$SiMe$_3$)$_2$] (Th−CH$_2$ = 2.48(2), 2.54(1) Å), Leznoff's diamido(ether) complex [(*^{DIPP}*NCOCN)Th(CH$_2$SiMe$_3$)$_2$] (*^{DIPP}*NCOCN = κ^3-{(ArNCH$_2$CH$_2$)$_2$O}$^{2-}$, Ar = 2,6-*^{i}*Pr$_2$C$_6$H$_3$; Th−CH$_2$ = 2.490(7), 2.513(8) Å),[14] Clark's aryloxide species [Th(OAr)$_2$(CH$_2$SiMe$_3$)$_2$] (Ar = 2,6-*^{t}*Bu$_2$C$_6$H$_3$; Th−CH$_2$ = 2.44(2), 2.49(2) Å)[23] and [Cp*Th(OAr)(CH$_2$SiMe$_3$)$_2$] (Ar = 2,6-*^{t}*Bu$_2$C$_6$H$_3$; Th−CH$_2$ = 2.460(9), 2.488(2) Å),[24] Mazzanti's 'salan' complex [(salan^{tBu2})Th(CH$_2$SiMe$_3$)$_2$] (salan^{tBu2} = κ^4-{*N,N'*-bis(2-methylene-4,6-di-*tert*-butylphenoxy)-*N,N'*-dimethyl-1,2-diami-noethane}; Th−CH$_2$ = 2.529(3) Å),[34] Arnold's macrocyclic [(TMTAA)(Cp*)Th(CH$_2$SiMe$_3$)] (TMTAA = κ^4-{6,8,15,17-tetramethyldibenzotetraaza[14]annulene]$^{2-}$; Th−CH$_2$ = 2.598(3) Å)[35] and amidinate species [{MeC(N*^{i}*Pr)$_2$}$_3$Th(CH$_2$SiMe$_3$)] (Th−CH$_2$ = 2.557(3) Å),[36] and Liddle's bis(iminophosphorane)-methandiide complex [(BIPM^{TMS})Th(CH$_2$SiMe$_3$)$_2$] (BIPM^{TMS} = κ^3-{C(PPh$_2$NSiMe$_3$)$_2$}$^{2-}$; Th−CH$_2$ = 2.51(2), 2.53(2) Å).[19]

The Th−C−Si angles of 119.8(1) and 129.6(2)° in dialkyl complex **4** are expanded relative to the ideal 109.5° angle, suggesting that the alkyl groups are engaged in α-agostic C−H−Th interactions.[12,23] This has been corroborated spectroscopically, whereby a $^1J_{C,H}$ coupling of 100 Hz was observed for the *CH$_2$*SiMe$_3$ groups in the ^{1}H-coupled ^{13}C NMR spectrum of **4** in C$_6$D$_6$ at room temperature. This coupling constant is significantly lower than typically expected for an sp^3-hybridized carbon atom, and compares well with values observed for related complexes.[37] It is also notable that in the solid state, a methylene carbon atom from each 1-adamantyl group approaches thorium relatively closely (Th−C(25) = 3.150(3) Å, Th−C(35) = 3.221(3) Å), raising the possibility of Th−H−C$_{Ad}$ γ-agostic interactions. However, such γ-agostic

interactions are not maintained in solution at room temperature, as a $^1J_{C,H}$ coupling of 124 Hz is observed for the NC*CH$_2$* groups of the freely-rotating 1-adamantyl substituents in the ^{1}H-coupled ^{13}C NMR spectrum of **4**, which is comparable to that for a typical sp^3-hybridized carbon atom[38] (the $^1J_{C,H}$ coupling constant for the NC*CH$_2$* environment of 1-adamantylamine in C$_6$D$_6$ is 126 Hz).

Unlike previously reported [(XA$_2$)Th(CH$_2$SiMe$_3$)$_2$], which can be dissolved in THF and recovered as a base-free species by evaporation of the solvent *in vacuo*,[10] the THF ligand of dialkyl complex **4** could not be removed from the solid *in vacuo*, or by dissolution in toluene and evaporation to dryness. Consequently, the steric influence of flanking 1-adamantyl substituents appears to be less than that of 2,6-diisopropylphenyl substituents. However, the thermal stability of **4** slightly exceeds that of [(XA$_2$)Th(CH$_2$SiMe$_3$)$_2$]; compound **4** showed no sign of decomposition after several hours at 85 °C, and decomposed over the course of 4.5 hours at 110 °C, whereas the THF-free XA$_2$ analogue is stable at 70 °C, but decomposed over several hours at 90 °C.[10] Both [(XA$_2$)Th(CH$_2$SiMe$_3$)$_2$] and **4** also catalyze intramolecular hydroamination, cyclizing H$_2$NCH$_2$CPh$_2$CH$_2$CH=CH$_2$ within 2 hours at 60 °C, and 17 hours at 70 °C, respectively, with 1 mol% catalyst loading in C$_6$D$_6$. However, this activity is far lower than that of [(XA$_2$)Ln(CH$_2$SiMe$_3$)(THF)] (Ln = Y[39] and Lu[40]).

To further explore the organometallic chemistry of thorium(IV) XAd complexes, we directed our attention towards bulky allyl ligands. Allyl complexes of thorium are rare; early efforts by Wilke and co-workers yielded the prototypical homoleptic tetra(allyl) species [Th(C$_3$H$_5$)$_4$], which the authors described as a yellow crystalline solid that decomposed at 0 °C.[41] Marks and co-workers later developed heteroleptic allyl complexes, such as the tris(cyclopentadienyl) thorium allyl complex [Cp$_3$Th(C$_3$H$_5$)], though neither [Th(C$_3$H$_5$)$_4$] nor [Cp$_3$Th(C$_3$H$_5$)] was structurally-characterized.[42] Crystallographically-authenticated examples of thorium allyl complexes are limited to Hanusa's homoleptic tetra(allyl) species [Th(allyl^{TMS})$_4$] {allyl^{TMS} = 1-(SiMe$_3$)C$_3$H$_4$} and [Th{1,3-(SiMe$_3$)$_2$C$_3$H$_3$}$_4$],[43] Evans' metallocene complex [Cp*$_2$Th(η^3-C$_3$H$_5$)(η^1-C$_3$H$_5$)],[44] and Walter and Zi's 'tuck-in' complex [(Cp'){η^5,η^1-(1,2-*^{t}*Bu$_2$-C$_5$H$_2$-4-(CMe$_2$CH$_2$)}Th{1-(Ph)C$_3$H$_4$}] (Cp' = {η^5-1,2,4-*^{t}*Bu$_3$(C$_5$H$_2$)}$^-$).[45]

Reaction of [(XAd)ThCl$_4$K$_2$]·x(dme) (**3**; x = 2) with 2.2 equiv of K[1-(SiMe$_3$)C$_3$H$_4$] (K[allyl^{TMS}]) at −78 °C in toluene afforded the diallyl complex [(XAd)Th(η^3-allyl^{TMS})$_2$] (**5**; Scheme 4). This dme-free complex was obtained as a vibrant yellow solid in approximately quantitative yield, and is highly soluble in ethereal, aromatic, and hydrocarbon solvents.

An X-ray crystal structure of **5**·2(toluene) (Figure 5) revealed an XAd thorium(IV) diallyl complex of approximate C_2 symmetry, with each allyl^{TMS} ligand adopting an η^3-bonding mode, coordinated above and below the plane of the XAd ligand, respectively. This bonding situation contrasts that in the bis(pentamethylcyclopentadienyl) thorium diallyl complex, [Cp*$_2$Th(η^3-C$_3$H$_5$)(η^1-C$_3$H$_5$)],[44] serving to highlight the extent to which the XAd dianion provides a much expanded coordination wedge[46] relative to two Cp* ligands. Furthermore, positioning

of the allyl ligands above and below the plane of the XAd pincer ligand differs from the bonding situation in previously reported [(XA$_2$)Th(η^2-CH$_2$Ph)(η^3-CH$_2$Ph)] and [(XA$_2$)Th{η^6-PhCH$_2$B(C$_6$F$_5$)$_3$}$_2$], in which one multihapto ligand is coordinated above the plane of the XA$_2$ ligand donor array, while the other is coordinated in the plane of the ligand.[17] This situation arises because (a) a readily accessible coordination site is available in the plane of the XA$_2$ ligand backbone, and (b) the flanking 2,6-diisopropylphenyl groups rotate so as to create an open coordination site above the plane of the xanthene backbone, simultaneously blocking off access to the coordination site below the plane of the ligand.
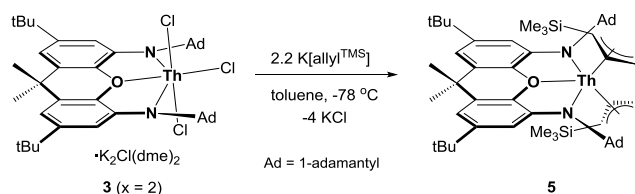
**Scheme 4**. Synthesis of [(XAd)Th(η^3-allyl^{TMS})$_2$] (**5**).
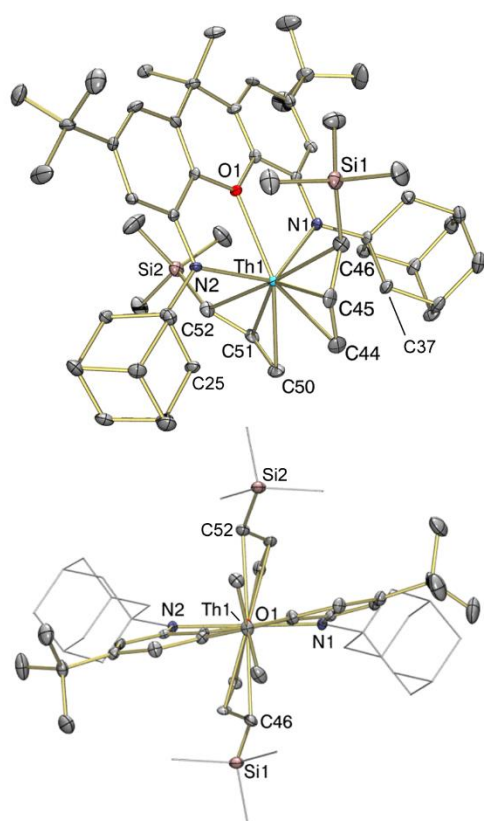
Figure 5. Two views of the X-ray crystal structure of [(XAd)Th(η^3-allyl^{TMS})$_2$]·2(toluene) (**5**·2(toluene)), with thermal ellipsoids at 50% probability. In both views, hydrogen atoms and toluene lattice solvent are omitted for clarity. In the bottom view, SiMe$_3$ methyl groups and 1-adamantyl groups are depicted in wireframe for clarity.

In XAd complex **5**, thorium resides only 0.03 Å out of the N/O/N-plane (cf. 0.33 Å in **4**), and the central oxygen-containing ring of

the xanthene backbone of XAd is approximately planar. However, the xanthene backbone is uniquely twisted in **5**, as illustrated by the angles between the N/O/N-plane and the planes formed by each individual aromatic ring of the ligand backbone; the plane of the arene ring bound to N(1) is tilted 11.6° relative to the N/O/N-plane, placing the arene above the N/O/N-plane, whereas the plane of the arene ring bound to N(2) is tilted 10.3° in the opposite direction, positioning this arene below the N/O/N-plane (Figure 5, view b).

Although thorium–ligand bond elongation might be expected in formally 7-coordinate **5**, the Th–N (2.375(6), 2.379(6) Å) and Th–O (2.492(5) Å) distances are equal within error (Th–N) or very slightly shorter (Th–O) than those in THF-coordinated dialkyl complex, **4**. The Th–C$_{allyl}$ distances range from 2.750(7) to 2.805(7) Å and are unremarkable, in line with Th–C$_{allyl}$ contacts observed in other thorium–η^3-allyl complexes, which range from 2.617(5)–2.984(6) Å).[43,45] The SiMe$_3$ substituent of each allyl ligand in **5** is in a *syn* position (Figure 6), and the central *meso*-carbon of each allyl ligand is tipped away from the metal, as illustrated by fold angles of 115.3 and 116.8°, respectively (fold angle = the angle between the plane of the three allyl carbon atoms and the plane passing through thorium and the two terminal allyl carbon atoms; Figure 6). This bonding situation mirrors that observed in [Th(allyl^{TMS})$_4$], in which all SiMe$_3$ groups are in *syn* positions, with allyl fold angles ranging from 119.8–121.4°.[43] Additionally, as with dialkyl complex **4**, a methylene carbon atom from each 1-adamantyl group of complex **5** approaches thorium relatively closely (Th–C(25) = 3.253(7) Å, Th–C(37) = 3.215(7) Å), potentially allowing for Th–H–C$_{Ad}$ agostic interactions in the solid state.
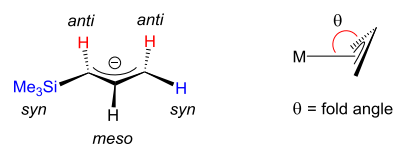

Figure 6. Naming of the chemical environments for the allyl^{TMS} substituents, and depiction of the fold angle of an η^3-allyl complex.

The room-temperature ^{1}H NMR spectrum of **5** in toluene-d_8 (Figure 7) is indicative of a C_2-symmetric isomer of [(XAd)Th(η^3-allyl^{TMS})$_2$], with resonances corresponding to the allyl protons and the 1-adamantyl NC(CH$_2$)$_3$ methylene protons broadened nearly completely into the baseline. The broadening observed for these resonances is attributed to dynamic allyl ligand behaviour, including averaging of the *syn* and *anti* protons of the allyl CH$_2$ group via rapid π–σ–π hapticity changes (Figure 8), as proposed for other thorium–allyl complexes.[42,43]

Indeed, upon heating a solution of **5** in toluene-d_8 to 87 °C, sharp ^{1}H NMR resonances corresponding to a single, averaged π-coordinated allyl ligand environment were observed. For example, the CH$_2$ protons of both allyl ligands appeared as a doublet integrating to 4H ($^3J_{H,H}$ = 11.8 Hz), the central *meso* proton environment afforded a multiplet (2H), the CH(SiMe$_3$) environment appeared as a doublet (2H; $^3J_{H,H}$ = 15.7 Hz), and the SiMe$_3$ protons gave rise to a singlet (18H).
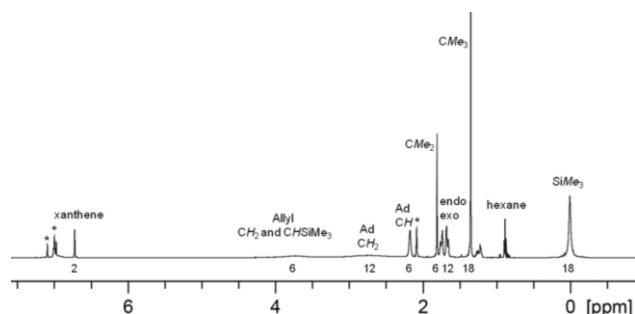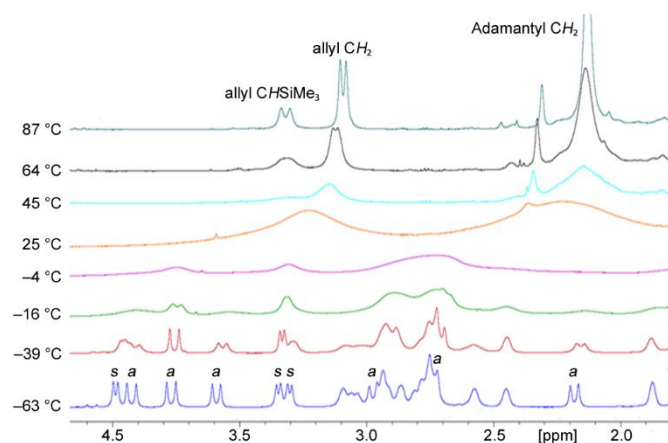
Figure 7. ^{1}H NMR spectrum of diallyl complex **5** in toluene-d_8 at room temperature (500 MHz). Numbers below the baseline indicate the approximate integration of each peak. * denotes toluene-d_7. The *meso*-CH resonance is broadened into the baseline and obscured by toluene-d_7 signals; the second xanthene CH peak is also obscured by toluene-d_7 signals.
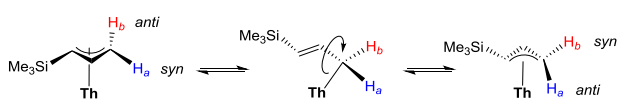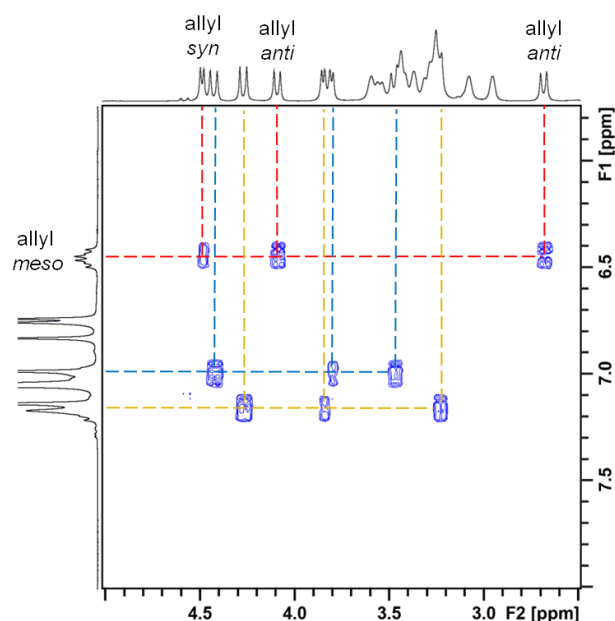

Figure 8. Exchange of the *geminal* H_a and H_b protons *via* a π–σ–π intramolecular conversion.

Figure 10. Selected region of the 2D [^{1}H–^{1}H] COSY NMR spectrum of diallyl complex **5** in toluene-d_8 at −63 °C (500 MHz), highlighting the presence of three unique η^3-allyl environments.

At low-temperature (−63 °C), a more complex ^{1}H NMR spectrum was observed (Figure 9), with three SiMe_3 peaks in an approximate 1:1:1 ratio, corresponding to multiple isomers with a total of 3 different allyl environments. Furthermore, the low-temperature 2D [^{1}H-^{1}H] COSY NMR spectrum conclusively identified 3 *meso*-CH environments, each one coupling to two *anti* and one *syn* proton resonance (Figure 10), with $^3J_{1H,1H}$ coupling constants of 16.1-18.4 Hz (trans) and 8.4-8.9 Hz (cis), respectively. These data are indicative of η^3-coordinated allyl ligands, with the SiMe_3 substituent in a *syn* position.

Figure 9. Variable temperature ^{1}H NMR spectra of **5** in toluene-d_8 between 87 and −63 °C, showing the allyl CHSiMe$_3$, allyl CH_2 and Adamantyl CH_2 region (500 MHz; a different sample was used for measurements above room temperature). In the spectrum at −63 °C, *syn*- and *anti*-allyl proton resonances are labelled 's' and 'a'.

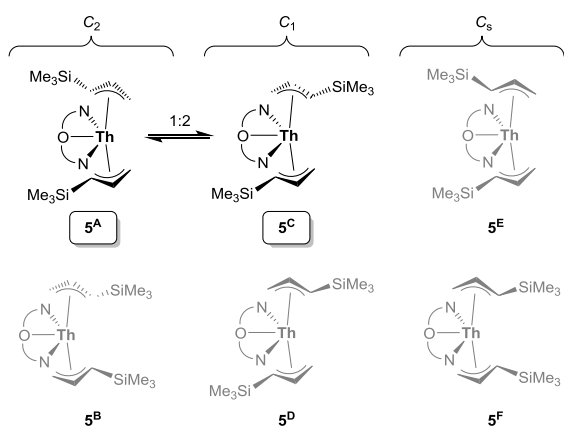Six possible isomers of compound **5**, all featuring exclusively η^3-coordinated allyl ligands, are depicted in Figure 11. Because an equal number of CMe_2, CMe_3, and SiMe_3 peaks are observed in the low-temperature ^{1}H and ^{13}C NMR spectra of **5** (although peak overlap cannot be excluded), the C_s-symmetric isomers, **5^E** and **5^F**, are unlikely to be major contributors, since they would give rise to one CMe_2, one SiMe_3, and two CMe_3 peaks. Additionally, isomers **5^E** and **5^F** are likely to be disfavored on steric grounds; both place the anti allyl protons of the two allyl ligands in the vicinity of a single 1-adamantyl substituent, and the latter also positions both silyl groups in close proximity to the 1-adamantyl substituents located in the plane of the XAd ligand. The low-temperature ^{1}H NMR spectrum of **5** must therefore result from a 1:2 mixture of a C_2 isomer (**5^A** or **5^B**; giving rise to one CMe_2, SiMe_3 and CMe_3 peak) and a C_1 isomer (**5^C** or **5^D**; giving rise to two CMe_2, SiMe_3 and CMe_3 peaks), respectively. Of the C_2 isomers, **5^A** is the structurally characterized isomer, so is likely to play a significant role in the solution chemistry of **5**. By contrast, **5^B** (like **5^F**) will undoubtedly be disfavored due to steric interactions between the SiMe_3 groups and the 1-adamantyl substituents in the plane of the XAd ligand. For the C_1-symmetric isomers, isomer **5^D** (like **5^E** and **5^F**) is likely to be disfavored since it positions both sets of *anti* allyl protons in the vicinity of a single 1-adamantyl substituent. Therefore, allyl complex **5** is posited to exist in solution as a 1:2 mixture of isomers **5^A** and **5^C**.

The original homoleptic tetra(allyl) complex [Th(C$_3$H$_5$)$_4$] suffered from limited thermal stability, decomposing at temperatures above 0 °C.[47] However, by replacing three allyl groups with cyclopentadienyl supporting ligands, the resulting heteroleptic thorium allyl complex [Cp$_3$Th(C$_3$H$_5$)] exhibited drastically improved thermal stability, decomposing at 210 °C.[42] The rigid XAd ancillary similarly serves to impart thermal

resilience in thorium allyl systems, as heteroleptic diallyl complex **5** can withstand heating at 85 °C for 15 hours, and was less than 5% decomposed after heating at 155 °C for 10 minutes.

Figure 11. Possible isomers of compound **5**. Based on the low temperature NMR spectra of **5**, isomers **5^A** and **5^C** are proposed to be present in solution in an approximate 1:2 ratio.

Summary and Conclusions

A new dianionic NON-donor pincer ligand, XAd, has been developed, featuring a rigid xanthene backbone with amido groups in the 4- and 5-positions, and N-(1-adamantyl) groups flanking the central coordination pocket. This ligand is an analogue of our previously reported XA$_2$ dianion, which features flanking N-(2,6-diisopropylphenyl) groups, and in order to evaluate the coordination properties of the XAd ligand, thorium(IV) dichloride, dialkyl, and diallyl complexes have been prepared. The thorium dichloro complex (**3**) was obtained via the salt metathesis reaction between [K$_2$(XAd)(dme)] (**2b**) and [ThCl$_4$(dme)$_2$], and contains 2 equivalents of occluded KCl. Reaction of **3** with 2 equiv of LiCH$_2$SiMe$_3$ or K(allyl^{TMS}) yielded [(XAd)Th(CH$_2$SiMe$_3$)$_2$(THF)] (**4**) and [(XAd)Th(η^3-allyl^{TMS})$_2$] (**5**), respectively.

The THF ligand in **4** is retained under vacuum, whereas the XA$_2$ analogue, [(XA$_2$)Th(CH$_2$SiMe$_3$)$_2$], can be dissolved in THF and recovered upon evaporation of the solvent *in vacuo*. These differences in reactivity illustrate the very different placement of steric bulk in the XAd and XA$_2$ ligands; in the plane of the xanthene ligand backbone in XAd, and above and below the plane of the ligand in XA$_2$, exerting an overall greater steric influence on co-ligand coordination in the case of the XA$_2$ ligand. However, the thermal stability of THF-coordinated **4** is greater than that of [(XA$_2$)Th(CH$_2$SiMe$_3$)$_2$].

The allyl ligands in **5** are both η^3-coordinated, but undergo rapid π-σ-π hapticity changes at room temperature and above. Additionally, low temperature NMR spectroscopy revealed an equilibrium between two isomers; a C_1-symmetric isomer and the crystallographically-characterized C_2 isomer. The combination of bulky allyl ligands with the rigid XAd ancillary imparts a high level of thermal stability, since **5** is stable at 85 °C, and was less than 5% decomposed after heating at 155 °C

for 10 minutes. This thermal stability far exceeds that of homoleptic [Th(allyl^{TMS})$_4$], which melts with decomposition at 88-90 °C.[43]

Experimental

General Procedures: General synthetic procedures have been reported elsewhere.[8-10,17,48] Deuterated solvents (C$_6$D$_6$, toluene-d_8, THF-d_8) were purchased from ACP Chemicals. [Th(NO$_3$)$_4$(H$_2$O)$_4$] was purchased from Strem Chemicals. Xanthone, ^{t}BuCl, anhydrous FeCl$_3$, Br$_2$, 1-adamantylamine, Me$_3$SiCl, NaO^{t}Bu, DPEPhos, Pd(OAc)$_2$, KO^{t}Bu, NaH, KH (30 wt.% in mineral oil), 3-(trimethylsilyl)propene (H[allyl^{TMS}]), LiCH$_2$SiMe$_3$ (1.0M in n-pentane), ^{s}BuLi (1.40 M in cyclohexane), and ^{n}BuLi (1.60 M in hexane) were purchased from Sigma-Aldrich. Prior to use, solid LiCH$_2$SiMe$_3$ was obtained by removal of pentane *in vacuo*, and solid KH was obtained by filtration and washing with hexanes. 1-adamantylamine was dried *in vacuo* prior to use, but the amine slowly sublimes under reduced pressure (<10 mTorr). Before use, all traces of moisture and ethanol were eliminated from H$_2$[XAd] by stirring with NaH (4 equiv) in toluene for 16 hours at room temperature, followed by filtration and evaporation to dryness *in vacuo*. 4,5-dibromo-2,7-di-*tert*-butyl-9,9-dimethylxanthene[49] and KCH$_2$Ph[50] were prepared using literature procedures. [ThCl$_4$(dme)$_2$] was prepared using two different methods: a modified version of the procedure reported by Gambarotta *et al.*,[49] and a modified version of the procedure reported by Kiplinger *et al*.[51] (by stirring [ThCl$_4$(H$_2$O)$_4$] with excess Me$_3$SiCl in dme for 12 h at 50 °C). K[1-(SiMe$_3$)C$_3$H$_4$] (K[allyl^{TMS}]) was prepared by lithiation of 3-(trimethylsilyl)propene (H[allyl^{TMS}]) using ^{s}BuLi, followed by transmetallation with KO^{t}Bu in THF at −78 °C.

Nuclear magnetic resonance spectroscopy (^{1}H, ^{13}C{^{1}H}, ^{13}C, uDEFT, DEPT-135, DEPTq, COSY, HSQC, HMBC) experiments were performed on Bruker AV-200, DRX-500 and AV-600 spectrometers. Spectra were obtained at 298 K unless otherwise specified. ^{1}H NMR and ^{13}C NMR spectra are referenced relative to SiMe$_4$ through a resonance of the employed deuterated solvent or proteo impurity of the solvent; C$_6$D$_6$ (δ 7.16 ppm), toluene-d_8 (δ 7.09, 7.01, 6.97, 2.08 ppm), and THF-d_8 (δ 3.58, 1.72 ppm) for ^{1}H NMR, and C$_6$D$_6$ (δ 128.06 ppm), toluene-d_8 (δ 137.48, 128.87, 127.96, 125.13, 20.43) and THF-d_8 (67.21, 25.31 ppm) for ^{13}C{^{1}H} NMR. For XAd, the numbering scheme (CH^{1,8}, C^{2,7}, CH^{3,6}, C^{4,5}, C^{10,13} and C^{11,12}) for the xanthene ligand backbone has been described previously.[16,28]

X-ray crystallographic analyses were performed on suitable crystals coated in Paratone oil and mounted on a SMART APEX II diffractometer with a 3 kW Sealed tube Mo generator in the McMaster Analytical X-Ray (MAX) Diffraction Facility. Data were typically collected at 100 K. Complex **5** was determined to be an inversion twin. Combustion elemental analyses were performed on a Thermo EA1112 CHNS/O analyzer by Ms. Meghan Fair or Dr. Steve Kornic of this department, and on a Carlo Erba EA 1110CHN elemental analyzer at Simon Fraser University by Mr. Farzad Haftbaradaran (with sample preparation conducted by Dr. Wen Zhou of the Leznoff research group at Simon Fraser University).

H$_2$[XAd]   (1): 4,5-dibromo-2,7-di-*tert*-butyl-9,9-dimethyl-xanthene (7.28 g, 15.16 mmol), 1-adamantylamine (4.59 g, 30.31 mmol), NaO^{t}Bu (4.08 g, 42.42 mmol), Pd(OAc)$_2$ (0.040 g,

0.18 mmol) and DPEPhos (0.142 g, 0.26 mmol) in toluene (~200 mL) were heated to 95 °C for 14 days. The cream-coloured reaction mixture was then quenched with water, extracted with toluene (3 × 20 mL), and dried over MgSO$_{4(s)}$ before removing volatiles *in vacuo*, yielding an oily cream-coloured solid. The solids were taken up in a refluxing ethanol/toluene mixture (~10:1), and upon cooling, H$_2$[XAd] (**1**) precipitated as a white solid (7.63 g, 12.29 mmol) in 81% yield. **¹H NMR (C$_6$D$_6$, 600.1 MHz, 298 K):** δ 7.27 (d, 2H, $^4J_{H,H}$ = 2.2 Hz, C$H^{3,6}$), 7.06 (d, 2H, $^4J_{H,H}$ = 2.2 Hz, C$H^{1,8}$), 4.20 (s, 2H, NH), 2.11 (d, 12H, $^3J_{H,H}$ = 2.6 Hz, Ad CH_2), 2.01 (br s, 6H, Ad CH), 1.70 (s, 6H, CMe_2), 1.59 (appt. q, 12H, $^2J_{H,H}$ = 11.7 Hz, Ad CH_2 *endo/exo*), 1.40 (s, 18H, CMe_3). **¹³C{¹H} NMR (C$_6$D$_6$, 150 MHz, 298 K):** δ 145.03 (CCMe$_3$), 139.64 (xanthene $C^{11,12}$), 134.32 (xanthene $C^{4,5}$), 130.0 (xanthene $C^{10,13}$), 114.91 (C$H^{3,6}$), 112.45 (C$H^{1,8}$), 52.59 (Ad NC), 44.25 (Ad CH_2), 36.92 (Ad *endo/exo*), 35.47 (CMe_2), 34.71 (CMe_3), 32.08 (CMe_2), 31.91 (CMe_3), 30.29 (Ad CH). **Anal. Calcd. For C$_{43}$H$_{60}$N$_2$O:** C, 83.17; H, 9.74; N, 4.51 %. Found: C, 83.25; H, 9.77; N, 4.41 %.

[{K(THF)$_3$}$_2$(XAd)] (2a) (*in situ*): A mixture of H$_2$[XAd] (0.020 g, 0.032 mmol), 4 equiv of KH (0.005 g, 0.129 mmol), and THF-d_8 (~0.6 mL) was sealed in a J-Young tube and heated to 65 °C. Immediately, H$_{2(g)}$ evolution began, and heating was continued for 3 days. Complete conversion of **1** to **2a** was verified by ¹H and ¹³C NMR. X-ray quality crystals of [{K(THF)$_3$}$_2$(XAd)] (**2a**) were obtained from THF/hexanes at −30 °C. However, **2a** readily de-solvated, in our hands with accompanying decomposition to yield proligand **1**. **¹H NMR (THF-d_8, 600.1 MHz, 298 K):** δ 6.24 (d, 2H, $^4J_{H,H}$ = 2.0 Hz, C$H^{3,6}$), 5.67 (d, 2H, $^4J_{H,H}$ = 2.0 Hz, C$H^{1,8}$), 2.08 (br s, 6H, Ad CH), 2.01 (br s, 12H, Ad CH_2), 1.73 (appt. t, 12H, $^2J_{H,H}$ = 14.6 Hz, Ad CH_2 *endo/exo*), 1.46 (s, 6H, CMe_2), 1.23 (s, 18H, CMe_3). **¹³C{¹H} NMR (THF-d_8, 150 MHz, 298 K):** δ 149.02 (xanthene $C^{4,5}$), 143.78 (CCMe$_3$), 137.97 (xanthene $C^{11,12}$), 127.26 (xanthene $C^{10,13}$), 106.84 (C$H^{3,6}$), 95.76 (C$H^{1,8}$), 52.66 (Ad NC), 45.07 (Ad CH_2), 38.73 (Ad *endo/exo*), 35.21 (CMe_2), 34.85 (CMe_3), 32.54 (CMe_2), 32.43 (CMe_3), 31.73 (Ad CH).

[K$_2$(XAd)(dme)] (2b) (*in-situ; preparatory scale*): *Method 1*: A mixture of H$_2$[XAd] (**1**; 0.500 g, 0.81 mmol), 2.5 equiv of KCH$_2$Ph (0.262 g, 2.0 mmol) and dme (60 mL) was stirred at −78 °C and then slowly warmed to room temperature; stirring was continued for a total of 12 h. The grey slurry was evaporated to dryness *in vacuo*, yielding an off-white solid. ¹H NMR spectroscopy (THF-d_8) confirmed the identity of crude product to be [K$_2$(XAd)(dme)] (**2b**), which was subsequently used without further purification.

Method 2: A mixture of H$_2$[XAd] (**1**; 0.500 g, 0.81 mmol), KH (0.071 g, 1.77 mmol), and dme (~35 mL) was stirred for ~ 1 week at room temperature, over which time a light pink precipitate formed. Volatiles were removed *in vacuo*, yielding a pale pink solid; ¹H NMR spectroscopy (THF-d_8) indicated complete conversion from proligand **1** to crude [K$_2$(XAd)(dme)] (**2b**), which was subsequently used without further purification. The ¹H NMR spectrum (THF-d_8) of isolated crude **2b** is identical to that of **2a** produced *in situ*, but with the addition of one equiv of free dme.

[(XAd)ThCl$_4$K$_2$]·x(dme) (3; x = 0.5-2): *Method A*: [K$_2$(XAd)(dme)] (**2b**) was first generated *in situ* via *Method 1* using 0.500 g (0.81 mmol) of H$_2$[XAd]. To the resulting solid **2b**, [ThCl$_4$(dme)$_2$] (0.446 g, 0.81 mmol) was added, and dme (50 mL) was condensed in at −78 °C. The mixture warmed to room temperature and was stirred for a total of 24 h. The white slurry was evaporated to dryness *in vacuo*, yielding a solid residue which was extracted with dme (25 mL) and centrifuged to remove any insoluble material. The mother liquors were evaporated to dryness, hexanes was added (60 mL), and the white slurry was sonicated. The solids were collected by filtration and washed with 3 × 15 mL hexanes to yield 0.647 g of [(XAd)ThCl$_4$K$_2$]·x(dme) (**3**) (0.517 mmol, 64 % yield) as a white solid powder. The amount of dme accompanying complex **3** varied by batch (ranging from 0.5 to 2 equiv).

Method B: [K$_2$(XAd)(dme)] (**2b**) was generated *in situ* via *Method 2* using 0.500 g (0.81 mmol) of H$_2$[XAd]. To the resulting solid **2b**, [ThCl$_4$(dme)$_2$] (0.446 g, 0.81 mmol) and THF (30 mL) were added. The resulting slurry was stirred for 48 h at room temperature, over which time the solution became pale yellow and copious white solids precipitated; volatiles were subsequently removed *in vacuo*. The solids were extracted with minimal dme, centrifuged to remove any insoluble material, and the mother liquors were removed *in vacuo* to yield a yellowish off-white solid. The solid was sonicated in hexanes, filtered, and washed with 3 × 15 mL hexanes to afford 0.200 g of [(XAd)ThCl$_4$K$_2$]·x(dme) (**3**; x = 1) as an off-white solid (0.172 mmol, 21% yield). The low yield is likely due to incomplete extraction with dme and subsequent loss of product during centrifugation. **¹H NMR** (using **3** (x = 1) prepared using *Method B*) **(THF-d_8, 600.1 MHz, 298 K):** δ 6.69 (d, 2H, $^4J_{H,H}$ = 1.7 Hz, C$H^{3,6}$), 6.58 (d, 2H, $^4J_{H,H}$ = 1.7 Hz, C$H^{1,8}$), 3.43 (s, 4H, free dme CH_2), 3.27 (s, 6H, free dme CH_3), 2.59 (br s, 12H, Ad CH_2), 2.24 (br s, 6H, Ad CH), 1.82 (appt. q, 12H, $^2J_{H,H}$ = 12.1 Hz, Ad CH_2 *endo/exo*), 1.62 (s, 6H, CMe_2), 1.30 (s, 18H, CMe_3). **¹³C{¹H} NMR (THF-d_8, 150 MHz, 298 K):** δ 146.47 (CCMe$_3$), 143.06 (xanthene $C^{4,5}$), 140.34 (xanthene $C^{11,12}$), 127.23 (xanthene $C^{10,13}$), 112.36 (C$H^{3,6}$), 109.73 (C$H^{1,8}$), 72.55 (free dme CH_2), 58.69 (free dme CH_3), 56.61 (Ad NC), 41.28 (Ad CH_2), 37.40 (Ad *endo/exo*), 35.09 (CMe_3), 34.56 (CMe_2), 33.93 (CMe_2), 31.73 (CMe_3), 30.77 (Ad CH). **Anal. Calcd. For C$_{47}$H$_{68}$N$_2$O$_3$ThCl$_4$K$_2$** (complex **3** (x = 1) prepared using *Method B*): C, 48.62; H, 5.90; N, 2.41 %. Found: C, 48.80; H, 6.09; N, 2.12 % (trial 1), and C, 48.89; H, 6.23; N, 2.08 % (trial 2). **Anal. Calcd. For C$_{51}$H$_{78}$N$_2$O$_5$ThCl$_4$K$_2$** (complex **3** (x = 2) prepared using *Method A*): C, 48.96; H, 6.28; N, 2.24 %. Found: C, 48.60; H, 5.95; N, 2.25 %.

[(XAd)Th(CH$_2$SiMe$_3$)$_2$(THF)] (4): The chloro precursor "[(XAd)ThCl$_2$]·x(THF)·y(KCl)" (**3'**) was first generated *in situ* in THF (45 mL) via *Method B* using 0.300 g (0.48 mmol) of H$_2$[XAd]. A separate flask was charged with solid LiCH$_2$SiMe$_3$ (0.093 g, 0.99 mmol) and THF (15 mL), and both solutions were cooled to 0 °C. The alkyllithium solution was added dropwise via cannula to the solution of *in situ*-generated **3'**. Upon complete addition, the mixture slowly warmed to room temperature and was stirred for an additional 12 h. The volatiles were removed *in vacuo*, yielding a grey solid, which was dissolved in toluene (10

mL) and centrifuged to remove insoluble KCl and LiCl salts. The golden-coloured mother liquors were removed *in vacuo* to afford an off-white solid, which was subsequently sonicated in hexanes, collected by filtration, and dried *in vacuo* to yield 0.128 g of **4** (0.117 mmol) as a white solid in 24% yield. The low yield is likely due to appreciable solubility of **4** in hexanes and the multi-stage nature of the reaction. X-Ray quality crystals of **4** were obtained from a saturated hexanes solution at −30 °C. **¹H NMR (C_6D_6, 600.1 MHz, 298 K):** δ 7.10 (br s, 2H, C*H*³,⁶), 6.75 (br s, 2H, C*H*¹,⁸), 3.46 (br s, 4H, coordinated THF C*H*₂²,⁵), 2.92 (br s, 12H, Ad C*H*₂), 2.36 (br s, 6H, Ad C*H*), 1.95, 1.76 (appt. d, 2 × 6H, $J_{H,H}$ = 11.9 Hz, Ad C*H*₂ *endo/exo*), 1.71 (s, 6H, C*Me*₂), 1.39 (s, 18H, C*Me*₃), 0.90 (br s, 4H, coordinated THF C*H*₂³,⁴), 0.33 (s, 18H, CH₂SiMe₃), 0.09 (s, 4H, C*H*₂SiMe₃). **¹³C{¹H} NMR (C_6D_6, 150 MHz, 298 K):** δ 146.40 (*C*CMe₃), 143.28 (xanthene *C*⁴,⁵), 141.97 (xanthene *C*¹¹,¹²), 128.90 (xanthene *C*¹⁰,¹³), 112.22 (*C*H³,⁶), 108.36 (*C*H¹,⁸), 85.68 (Th*C*H₂SiMe₃), 70.36 (coordinated THF *C*H₂²,⁵), 57.22 (Ad N*C*), 41.02 (Ad *C*H₂), 37.27 (Ad *endo/exo*), 34.96 (*C*Me₃), 34.37 (*C*Me₂), 32.72 (C*Me*₂), 31.91 (C*Me*₃), 30.22 (Ad *C*H), 25.08 (coordinated THF *C*H₂³,⁴), 4.65 (ThCH₂Si(*C*H₃)₃). **¹H NMR (toluene-d_8, 500.1 MHz, 197 K):** δ 7.13 (br s, 2H, C*H*³,⁶), 6.78 (br s, 2H, C*H*¹,⁸), 3.56, 3.32, 1.87 (br s, 3 × 4H, Ad C*H*₂), 3.38 (br s, 4H, coordinated THF C*H*₂²,⁵), 2.69, 2.27, 2.21 (br s, 3 × 2H, Ad C*H*), 2.00, 1.72 (br m, 2 × 6H, Ad C*H*₂ *endo/exo*), 1.87, 1.61 (br s, 2 × 3H, C*Me*₂), 1.41 (s, 18H, C*Me*₃), 0.65 (br s, 4H, coordinated THF C*H*₂³,⁴), 0.55, 0.39 (s, 2 × 9H, CH₂SiMe₃), 0.50, −0.18 (br s, 2 × 2H, C*H*₂SiMe₃). **¹³C{¹H} NMR (toluene-d_8, 125 MHz, 197 K):** δ 145.69 (*C*CMe₃), 142.99 (xanthene *C*⁴,⁵), 141.44 (xanthene *C*¹¹,¹²), 128.14 (xanthene *C*¹⁰,¹³), 112.00 (*C*H³,⁶), 107.94 (*C*H¹,⁸), 85.35, 84.71 (2 × Th*C*H₂SiMe₃), 70.85 (coordinated THF *C*H₂²,⁵), 57.05 (Ad N*C*), 42.04, 41.74, 38.70 (3 × Ad *C*H₂), 37.14, 37.07, 36.01 (3 × Ad *endo/exo*), 34.79 (*C*Me₃), 34.74, 29.60 (2 × C*Me*₂), 34.13 (*C*Me₂), 31.65 (C*Me*₃), 29.89, 29.60 (3 × Ad *C*H), 24.68 (coordinated THF *C*H₂³,⁴), 4.77, 4.66 (2 × ThCH₂Si(*C*H₃)₃). **Anal. Calcd. For $C_{55}H_{88}N_2O_2Si_2Th$:** C, 60.19; H, 8.08; N, 2.55 %. Found: C, 60.48; H, 7.89; N, 2.53 %.

[(XAd)Th(η³-allyl^{TMS})₂] (5): A mixture of [(XAd)ThCl₄K₂]·2(dme) (**3**; *x* = 2) (0.130 g, 0.104 mmol) and approximately 3 equiv of K[allyl^{TMS}] (0.049 g, 0.319 mmol) in toluene (35 mL) was stirred at −78 °C and then warmed slowly to room temperature; stirring was continued for a total of 24 h. Upon initial introduction of the toluene solvent, the solution became a bright yellow colour. After 24 h of stirring, the solvent was removed *in vacuo* to afford a bright yellow solid residue. The residue was extracted with O(SiMe₃)₂ (10 mL), and insoluble material (KCl) was removed by centrifugation. The yellow mother liquors were evaporated to dryness *in vacuo*, yielding 0.112 g of diallyl complex **5** as a vibrant yellow solid (0.104 mmol, 100% yield; the slightly low carbon elemental analysis may indicate that small amounts of KCl remain in the isolated sample). Alternatively, **5**·0.5(*n*-pentane) could be obtained by recrystallizing **5** from *n*-pentane at −30 °C. X-ray quality crystals of **5**·2(toluene) were obtained from toluene/hexanes at −30 °C. **¹H NMR (toluene-d_8, 500.1 MHz, 298 K):** δ 6.97 (v. br s, 2H, *meso*-allyl CH₂C*H*), 6.72 (d, $^4J_{H,H}$ = 1.59 Hz, 2H, C*H*¹,⁸/C*H*³,⁶), 3.72 (v. br s, 6H, *anti*-allyl-C*H*SiMe₃ + *gem*-allyl-C*H*₂), 2.73 (v. br s, 12H, Ad C*H*₂), 2.17 (br s, 6H, Ad C*H*),

1.80 (s, 6H, C*Me*₂), 1.70 (m, 12H, Ad *endo/exo*), 1.35 (s, 18H, C*Me*₃), 0.00 (br s, 18H, allyl-CHSi*Me*₃). **¹H NMR (toluene-d_8, 500.1 MHz, 350 K):** δ 6.94 (d, $^4J_{H,H}$ = 2.03 Hz, 2H, C*H*³,⁶), 6.92 (m, 2H, *meso*-allyl CH₂C*H*), 6.69 (d, $^4J_{H,H}$ = 2.03 Hz, 2H, C*H*¹,⁸), 3.81 (br d, $^3J_{H,H}$ = 15.7, 2H, *anti*-allyl-C*H*SiMe₃), 3.60 (br d, $^3J_{H,H}$ = 11.8, 4H, *gem*-allyl-C*H*₂), 2.63 (br s, 12H, Ad-C*H*₂), 2.17 (br s, 6H, Ad C*H*), 1.76 (s, 6H, C*Me*₂), 1.70 (m, 12H, Ad *endo/exo*), 1.33 (s, 18H, C*Me*₃), −0.05 (s, 18H, allyl-CHSi*Me*₃). **¹³C{¹H} NMR (toluene-d_8, 125 MHz, 350 K):** δ 159.16 (*meso*-allyl-CH₂*C*H), 146.53 (*C*CMe₃), 143.14 (xanthene *C*⁴,⁵), 141.49 (xanthene *C*¹¹,¹²), 128.60 (xanthene *C*¹⁰,¹³), 112.14 (*C*³,⁶), 110.23 (*C*¹,⁸), 96.80 (allyl-*C*HSiMe₃), 86.17 (*gem*-allyl-*C*H₂), 57.89 (Ad N*C*), 40.27 (Ad *C*H₂), 37.64 (Ad *endo/exo*), 35.10 (*C*Me₃), 34.17 (*C*Me₂), 34.05 (C*Me*₂), 31.91 (C*Me*₃), 30.29 (Ad *C*H), 1.00 (allyl-CHSi*Me*₃). **¹H NMR (toluene-d_8, 500.1 MHz, 210 K, select resonances):** δ 6.46 (m, 1H, *meso*-allyl-CH₂C*H*), 4.49, 3.85, 3.80 (d, 3 × 1H, $^3J_{cis-H,H}$ = 8.4–8.9 Hz, allyl *syn*-C*H*₂), 4.43, 4.27, 4.09, 2.68 (d, 4 × 1H, $^3J_{trans-H,H}$ = 16.1–18.4 Hz, allyl *anti*-C*H*₂ + allyl *anti*-C*H*SiMe₃), 1.90, 1.89, 1.88 (s, 3 × 3H, C*Me*₂), 1.41, 1.36, 1.35, (s, 3 × 9H, C*Me*₃), 0.28, 0.02, −0.03 (s, 3 × 9H, allyl-CHSi*Me*₃). **Anal. Calcd. For $C_{55}H_{84}N_2OSi_2Th$:** C, 61.31; H, 7.86; N, 2.60 %. Found: C, 60.67; H, 7.57 ; N, 2.53 %.

Acknowledgements

References

1   D. W. Keogh, in Actinides: Inorganic & Coordination Chemistry - Encyclopedia of Inorganic Chemistry, ed. R. B. King, R. H. Crabtree, John Wiley & Sons: Chichester, England, 2005; vol. 1, pp. 2.

2   C. J. Burns, D. L. Clark and A. P. Sattelberger, in Actinides: Organometallic Chemistry - Encyclopedia of Inorganic Chemistry, ed. R. B. King, C. M. Lukehart, John Wiley & Sons: Chichester, England, 2005; vol. 1, pp. 33.

3   (a) T. Andrea and M. S. Eisen, *Chem. Soc. Rev.*, 2008, **37**, 550; (b) A. R. Fox, S. C. Bart, K. Meyer and C. C. Cummins, *Nature*, 2008, **455**, 341.

4   (a) I. S. R. Karmel, R. J. Batrice and M. S. Eisen, *Inorganics*, 2015, **3**, 392; (b) E. Barnea and M. S. Eisen, *Coord. Chem. Rev.*, 2006, **250**, 855.

5   (a) M. S. Eisen and T. J. Marks, *J. Mol. Catal.*, 1994, **86**, 23; (b) M. S. Eisen and T. J. Marks, *Organometallics*, 1992, **11**, 3939.

6   T. J. Marks and V. W. Day, in Actinide Hydrocarbyl and Hydride Chemistry - Fundamental and Technological Aspects of Organo-f-Element Chemistry, ed. T. J. Marks, I. L. Fragalà, D. Reidel Publishing Company: Dordrecht, 1985; pp. 115.

7   (a) Â. Domingos, N. Marques, A. P. de Matos, I. Santos and M. Silva, *Organometallics*, 1994, **13**, 654; (b) E. M. Matson, W. P.

Forrest, P. E. Fanwick and S. C. Bart, *Organometallics*, 2013, **32**, 1484.

8 C. A. Cruz, D. J. H. Emslie, H. A. Jenkins and J. F. Britten, *Dalton Trans.*, 2010, **39**, 6626.

9 C. A. Cruz, D. J. H. Emslie, C. M. Robertson, L. E. Harrington, H. A. Jenkins and J. F. Britten, *Organometallics*, 2009, **28**, 1891.

10 C. A. Cruz, D. J. H. Emslie, L. E. Harrington, J. F. Britten and C. M. Robertson, *Organometallics*, 2007, **26**, 692.

11 S. Duhović, S. Khan and P. L. Diaconescu, *Chem. Commun.*, 2010, **46**, 3390.

12 K. C. Jantunen, F. Haftbaradaran, M. J. Katz, R. J. Batchelor, G. Schatte and D. B. Leznoff, *Dalton Trans.*, 2005, 3083.

13 C. E. Hayes and D. B. Leznoff, *Organometallics*, 2010, **29**, 767.

14 C. E. Hayes, R. H. Platel, L. L. Schafer and D. B. Leznoff, *Organometallics*, 2012, **31**, 6732.

15 K. C. Jantunen, R. J. Batchelor and D. B. Leznoff, *Organometallics*, 2004, **23**, 2186.

16 N. R. Andreychuk, S. Ilango, B. Vidjayacoumar, D. J. H. Emslie and H. A. Jenkins, *Organometallics*, 2013, **32**, 1466.

17 C. A. Cruz, D. J. H. Emslie, L. E. Harrington and J. F. Britten, *Organometallics*, 2008, **27**, 15.

18 (a) E. L. Lu, O. J. Cooper, J. McMaster, F. Tuna, E. J. L. McInnes, W. Lewis, A. J. Blake and S. T. Liddle, *Angew. Chem. Int. Ed.*, 2014, **53**, 6696; (b) E. L. Lu, O. J. Cooper, F. Tuna, A. J. Wooles, N. Kaltsoyannis and S. T. Liddle, *Chem. Eur. J.*, 2016, **22**, 11559.

19 M. Gregson, E. Lu, D. P. Mills, F. Tuna, E. J. L. McInnes, C. Hennig, A. C. Scheinost, J. McMaster, W. Lewis, A. J. Blake, A. Kerridge and S. T. Liddle, *Nat. Commun.*, 2017, **8**, 14137.

20 The 1,1'-bis(amido)ferrocene ligand in [LUR₂] complexes could also be considered to be tridentate if a weak iron-uranium interaction is included in the bonds formed between the ligand and the metal; M. J. Monreal and P. L. Diaconescu, *Organometallics*, **2008**, *27*, 1702.

21 (a) M. Silva, N. Marques and A. P. de Matos, *J. Organomet. Chem.*, 1995, **493**, 129; (b) M. P. C. Campello, M. J. Calhorda, Â. Domingos, A. Galvão, J. P. Leal, A. P. de Matos and I. Santos, *J. Organomet. Chem.*, 1997, **538**, 223; (c) E. M. Matson, M. G. Crestani, P. E. Fanwick and S. C. Bart, *Dalton Trans.*, 2012, **41**, 7952.

22 N. R. Andreychuk, D. J. H. Emslie, H. A. Jenkins and J. F. Britten, *J. Organomet. Chem.*, 2018, **857**, 16.

23 D. L. Clark, S. K. Grumbine, B. L. Scott and J. G. Watkin, *Organometallics*, 1996, **15**, 949.

24 R. J. Butcher, D. L. Clark, S. K. Grumbine, B. L. Scott and J. G. Watkin, *Organometallics*, 1996, **15**, 1488.

25 C. M. Fendrick, L. D. Schertz, V. W. Day and T. J. Marks, *Organometallics*, 1988, **7**, 1828.

26 For the synthesis of *N*-mesityl and *N*-cyclohexyl substituted 4,5-bis(amido)xanthene ligands, and the preparation of titanium(IV) bis(amido) and dibenzyl complexes, see: Porter, R. M.; Danopoulos, A. A. *Polyhedron* **2006**, *25*, 859.

27 The τ parameter is a structural descriptor for 5-coordinate complexes indicating the degree of trigonality; $\tau = (\beta - \alpha)/60$, where β and α are the two greatest bond angles in the complex (β>α). For a perfectly square-pyramidal geometry, τ = 0, while for a perfectly trigonal-bipyramidal geometry, τ = 1. See: A. W. Addison, T. N. Rao, J. Reedijk, J. van Rijn, G. C. Verschoor, *J. Chem. Soc. Dalton Trans.*, **1984**, 1349-1356.

28 B. Vidjayacoumar, S. Ilango, M. J. Ray, T. Chu, K. B. Kolpin, N. R. Andreychuk, C. A. Cruz, D. J. H. Emslie, H. A. Jenkins and J. F. Britten, *Dalton Trans.*, 2012, **41**, 8175.

29 C. E. Hayes, Y. Sarazin, M. J. Katz, J. F. Carpentier and D. B. Leznoff, *Organometallics*, 2013, **32**, 1183.

30 B. D. Stubbert and T. J. Marks, *J. Am. Chem. Soc.*, 2007, **129**, 6149.

31 CCSD accessed January 2018.

32 B. M. Gardner, W. Lewis, A. J. Blake and S. T. Liddle, *Organometallics*, 2015, **34**, 2386.

33 J. W. Bruno, T. J. Marks and V. W. Day, *J. Organomet. Chem.*, 1983, **250**, 237.

34 E. Mora, L. Maria, B. Biswas, C. Camp, I. C. Santos, J. Pecaut, A. Cruz, J. M. Carretas, J. Marcalo and M. Mazzanti, *Organometallics*, 2013, **32**, 1409.

35 S. Hohloch, M. E. Garner, B. F. Parker and J. Arnold, *Dalton Trans.*, 2017, **46**, 13768.

36 N. S. Settineri, M. E. Garner and J. Arnold, *J. Am. Chem. Soc.*, 2017, **139**, 6261.

37 J.-Y. Liu, Y. Zheng, Y.-G. Li, L. Pan, Y.-S. Li and N.-H. Hu, *J. Organomet. Chem.*, 2005, **690**, 1233.

38 J. W. Bruno, G. M. Smith, T. J. Marks, C. K. Fair, A. J. Schultz and J. M. Williams, *J. Am. Chem. Soc.*, 1986, **108**, 40.

39 K. S. A. Motolko, D. J. H. Emslie and H. A. Jenkins, *Organometallics*, 2017, **36**, 1601.

40 K. S. A. Motolko, D. J. H. Emslie and J. F. Britten, *RSC Advances*, 2017, **7**, 27938.

41 G. Wilke, B. Bogdanovic, P. Hardt, P. Heimbach, W. Keim, M. Kroner, W. Oberkirch, K. Tanaka, E. Steinrucke, D. Walter and H. Zimmermann, *Angew. Chem. Int. Ed. Engl.*, 1966, **5**, 151.

42 T. J. Marks and W. A. Wachter, *J. Am. Chem. Soc.*, 1976, **98**, 703.

43 C. N. Carlson, T. P. Hanusa and W. W. Brennessel, *J. Am. Chem. Soc.*, 2004, **126**, 10550.

44 R. R. Langeslay, J. R. Walensky, J. W. Ziller and W. J. Evans, *Inorg. Chem.*, 2014, **53**, 8455.

45 B. Fang, L. Zhang, G. H. Hou, G. F. Zi, D. C. Fang and M. D. Walter, *Chem. Sci.*, 2015, **6**, 4897.

46 In the chemistry of bent metallocene complexes, the "coordination wedge" describes the region between the two cyclopentadienyl ligands that is accessible to co-ligands. Therefore, in the comparison of XAd diallyl complex **5** with [Cp*₂Th(η³-C₃H₅)(η¹-C₃H₅)], the "coordination wedge" refers to the region between the two anionic Cp* or amido donors.

47 G. Wilke, B. Bogdanović, P. Hardt, P. Heimbach, W. Keim, M. Kröner, W. Oberkirch, K. Tanaka, E. Steinrücke, D. Walter and H. Zimmermann, *Angewandte Chemie International Edition in English*, 1966, **5**, 151.

48 C. A. Cruz, T. Chu, D. J. H. Emslie, H. A. Jenkins, L. E. Harrington and J. F. Britten, *J. Organomet. Chem.*, 2010, **695**, 2798.

49 J. S. Nowick, P. Ballester, F. Ebmeyer and J. Julius Rebek, *J. Am. Chem. Soc.*, 1990, **112**, 8902.

50 P. L. Bailey, R. A. Coxall, C. M. Dick, S. Fabre, L. C. Henderson, C. Herber, S. T. Liddle, D. Lorono-Gonzalez, A. Parkin and S. Parsons, *Chem. Eur. J.*, 2003, **9**, 4820.

51 T. Cantat, B. L. Scott and J. L. Kiplinger, *Chem. Commun.*, 2010, **46**, 919.